Title: Parallel functional subnetworks embedded in the macaque face patch system

Authors: Soo Hyun Park[1]*, Kenji W. Koyano[1], Brian E. Russ[1]†‡§, Elena N. Waidmann[1]¶, David B. T. McMahon[1]#, David A. Leopold[12]*

Affiliations:

[1]Section on Cognitive Neurophysiology and Imaging, National Institute of Mental Health; Bethesda, USA.

[2]Neurophysiology Imaging Facility, National Institute of Mental Health, National Institute of Neurological Disorders and Stroke, National Eye Institute; Bethesda, USA.

†Center for Biomedical Imaging and Neuromodulation, Nathan Kline Institute; Orangeburg, USA.

‡Department of Neuroscience, Icahn School of Medicine at Mount Sinai; New York City, USA.

§Department of Psychiatry, New York University at Langone; New York City, USA.

¶Laboratory of Neurogenetics of Language, The Rockefeller University; New York City, USA.

#Neuronal Networks Section, National Eye Institute; Bethesda, USA.

*Corresponding author. Email: soohyun.park@nih.gov, leopoldd@mail.nih.gov

Abstract: During normal vision, our eyes provide the brain with a continuous stream of useful information about the world. How visually specialized areas of the cortex, such as face-selective patches, operate under natural modes of behavior is poorly understood. Here we report that, during the free viewing of videos, cohorts of face-selective neurons in the macaque cortex fractionate into distributed and parallel subnetworks that carry distinct information. We classified neurons into functional groups based on their video-driven coupling with fMRI time courses across the brain. Neurons from each group were distributed across multiple face patches but intermixed locally with other groups at each recording site. These findings challenge prevailing views about functional segregation in the cortex and underscore the importance of naturalistic paradigms for cognitive neuroscience.

One-Sentence Summary: Natural visual experience reveals parallel functional subnetworks of neurons embedded within the macaque face patch system

Main Text: Face patches in the temporal cortex of macaques are spatially separate, densely interconnected (*1, 2*) regions, defined by their shared preference for faces (*3, 4*). Similar regions exist in the cortex of humans (*5*) and marmosets (*6*), suggesting this functional network is a conserved feature in primates (*7–9*). Individual patches differ in their neural response selectivity to facial attributes, such as viewpoint, identity, movement and expression (*10–12*). These differences have prompted speculation that face patches are arranged in one or more functional hierarchies (*13–15*).

Knowledge about the organization of the macaque face network derives principally from neural responses to briefly presented images. However, a few studies have begun to characterize the brain's responses to freely viewed natural videos (*16–20*), with some evidence suggesting that the basic layout of the face patch network is preserved under these conditions (*17*). While naturalistic paradigms sacrifice precise control over visual stimulation, they are able to more closely approximate the conditions under which the visual specialization evolved in the primate brain (*21*). An important question is whether the principles derived from image responses will extend to more natural modes of vision (*22*).

Here we approach this question using a combination of methods that offers a new perspective on the visual responses of face-selective neurons. Briefly, we describe the activity of isolated single neurons in multiple nodes of the macaque face patch network during the free and repeated viewing of videos depicting natural social behaviors. Rather than taking the conventional approach of analyzing a neuron's representation of visual features, we instead compare each neuron's activity to corresponding fMRI responses across the brain obtained to the same video. (**Fig. 1A**). Thus, each neuron is characterized through its cortical network profile, summarized as a map of positive and negative covariations, rather than through its explicit stimulus selectivity. This approach provides a robust, data-driven method to assess the functional organization of the face patch system amid the complexity of naturalistic stimuli, in the context of the whole-brain network.

To begin, we identified face patches in eleven behaving macaques using standard fMRI methods (*4, 17*). In nine animals, chronic microwire bundles were inserted into one or two of the four patches featured in the present study (**Fig. 1A**, see **Methods**). Each bundle consisted of flexible microwires that covered a small volume of tissue (< 1 mm^3) and allowed us to record the activity of isolated neurons across multiple daily sessions (*16, 23*). We then recorded responses from 389 single neurons across four fMRI-defined face patches (**Fig. 1B – C**; n = 33 from middle lateral, ML, n = 224 from anterior fundus, AF, n = 77 from posterior portion anterior medial, pAM, n = 55 from anterior portion of anterior medial, aAM face patches; see **Methods** for distinction between pAM and aAM). For each neuron, we recorded the spiking time courses elicited during the repeated free viewing of naturalistic videos. For 254 of the recorded neurons, we independently measured basic category selectivity to briefly presented images of faces, objects, and other categories. Of these neurons, 166 (65%) were determined to be face-selective (see **Methods**).

Throughout the population, neighboring neurons in each face patch exhibited diverse response time courses to the same video content (see **Fig. S1A** for the time courses of all neurons in the study). In agreement with previous recordings from face patch AF (*16*), the time courses of neighboring neurons in all patches often diverged markedly, despite sharing some temporal features, even among the 166 neurons demonstrated to be face selective in separate testing (**Fig. S1A – B**). Importantly, neurons sampled from different face patches, typically several millimeters apart, often responded with very similar time courses (**Fig. S1A and C**). Together,

these initial observations suggested that face-selective neurons exhibit a diversity of responses during natural modes of vision that are not segregated into distinct patches.

To explore this finding further, we applied the intermodal technique of single-unit fMRI mapping developed previously (*24*), which summarizes complex video-driven single-unit activity as a functional map of activity correlations across the brain (**Fig. 1D**). Each neuron's unique pattern of positive and negative activity correlations sheds light on its participation in different functional brain networks under natural viewing conditions. Methodologically, this approach overlaps with paradigms mapping spontaneous neural activity using intermodal methods (*25–27*). However, in this case, correlations are driven by an external video stimulus, followed by extensive averaging across presentations, and experiments were carried out across the brains of different individuals. Thus, our method is designed to eliminate components of spontaneous or otherwise trial-unique activity and is distinctly different from conventional functional connectivity.

The temporal structure of the 15-minute natural video served as a shared timeline for electrophysiological and fMRI data collected in different animals. Response time courses were averaged across multiple video presentations, both for individual neurons (8 – 15 presentations) and for the fMRI responses (28 – 40 presentations). This averaging, combined with the inherent reproducibility observed in both modalities (*16, 17*), provided excellent estimations of the mean response time course for both neurons and voxels (also see **Fig. S1D** for examples). We focus here on the correlation of average spiking time courses with cortical voxels, only noting that structures outside the cerebral cortex, including the superior colliculus, pulvinar, striatum, amygdala, and cerebellum, were also engaged (see ref. (*24*)).

The correlation maps derived from each face patch were strikingly diverse, consistent with a previous application of this method to face patch AF (*24*). An example of one neuron's map is shown in **Figure 2A**, where the fMRI coupling is depicted on a flattened cortical hemisphere. This neuron was recorded from face patch aAM and determined to be face-selective in separate testing (**Fig. 2A**, inset). This cortical correlation profile exhibited peaks that roughly matched the location of face patches, mapped in separate experiments (**Fig. 2A**, black lines, see **Methods**), suggesting the visual operation performed by this neuron can be related to modes of visual analysis that are largely restricted to other face patches.

The cortical correlation pattern shown in the example in **Figure 2A** was relatively common among face patch neurons, with similar examples shown from each of the four face patches in the top row of **Figure 2B**. At the same time, the columns in **Figure 2B** show that neurons with very different cortical correlation profiles were found within each of the four face patches. Dissimilar functional profiles were, for example, commonly observed among pairs of neurons recorded simultaneously from the same patch and even from the same electrode (see **Fig. S2**). Together, the rows and columns in **Figure 2B** illustrate that distinct neural subtypes were intermixed locally but shared across different face patches. For instance, each face patch contained neurons whose visual responses were broadly anticorrelated with visual areas but positively correlated with the retrosplenial cortex (**Fig. 2B**, second row), potentially suggesting that these neurons are influenced by the default mode network (*28, 29*). Each face patch also contained neurons whose activity was correlated with the foveal retinotopic cortex (**Fig. 2B**, third row), and others whose activity was correlated with dorsal stream visual areas in caudal superior temporal sulcus, intraparietal sulcus, and arcuate sulcus (**Fig. 2B**, fourth row), possibly linking to attentional network (*30, 31*). Notably absent in our analysis was any indication of

elevated local fMRI correlation in the vicinity of the neural recording sites. Thus multiple, highly distinct functional profiles were shared across each of the four face patches.

We next performed a population analysis of functional profiles obtained across the four face patches. We focused on neurons determined to be face selective in separate testing (**Fig. 3**; see **Fig. S5** for the results of similar analysis applied to the entire population). To succinctly summarize the important information derived from each neuron's correlation map, we delineated a set of 37 functional regions of interest (fROIs). For this, we identified continuous clusters of voxels across the cortical sheet that exhibited substantial correlations across all recorded neurons (see **Methods**; see **Fig. S3** for correspondence with atlas). This step allowed the correlation profile of each neuron to be expressed as a 37-element vector of value, with each element pertaining to the average correlation value within one fROI.

Correlation profiles for all face-selective neurons are shown in **Figure 3A**, sorted by their recording locations. Consistent with **Figure 2B**, this figure highlights the heterogeneous composition of face cells within each patch, with marked local intermixing of neural responses to the video stimulus. To better highlight the functional groups within this matrix, we applied unsupervised (K-means) clustering to the fMRI correlation maps of the population of face-selective cells (see **Methods** and **Fig. S4**). The optimization of the clustering suggested six functional subpopulations, which we termed cell groups *g1* - *g6*. When the neural profiles were reordered based on this clustering (**Fig. 3B**), it was plain that each functional subpopulation was contributed by neurons inhabiting multiple face patches.

To better aid visualization of the functional profiles of the different cell groups, we remapped the average fROI correlation vectors from each cell group back onto the flattened brain (**Fig. 3C**). The resulting maps revealed each cell group's specific regional coupling with the fMRI signal during naturalistic viewing. For example, one group of neurons showed relatively selective coupling to a subset of face patches, face patch AL, AD, and orbitofrontal areas (group *g1*), whereas neurons in another group (group *g4*) showed networks that appear to be complementary to the ones of group *g1*, featuring selective correlation to areas in the lower bank of STS. Another group was correlated strongly with areas in the STS and primary visual areas (group *g3*), while another (group *g6*) correlated strongly with eccentric portions of primary visual cortex in addition to the areas coupled with the group *g1*. While individual neurons composing each group differed somewhat in their specific profiles, this grouping provided an effective summary of the fMRI correlation patterns across the face-selective neural population.

Across the four patches, most functional cell groups were represented, although they were not evenly distributed (**Fig. 3D**), likely reflecting a degree of specialization of individual patches. For example, functional group *g5* with a broad, strong positive correlation profile was not observed among face-selective neurons recorded in patch aAM, nor was group *g6*. Groups *g3* and *g5*, two groups coupled strongly with STS regions, were more prominent among face-selective neurons recorded from STS face patches (ML and AF), whereas group g1 with selective face-patch correlation was observed more in face neurons from the more ventral patches (pAM and aAM).

These findings shed new light on the division of labor among single neurons within a functionally defined cortical network. They suggest that, under stimulation conditions that approximate natural vision, individual face patches are neither functionally homogeneous nor apparently arranged in a hierarchical progression. Instead, face patches overlap markedly in their functional composition. The data thus suggest the face patch system is composed of parallel

threads of neural subnetworks, intermixed at a local level and carrying out distinct types of visual operations across multiple nodes of the network (**Fig. 4**).

The extreme mixing of signals in each face patch is surprising, given the common view that face patches are a clear example of domain-specificity in the brain. While this traditional view is supported by many experiments, it evidently does not extend to more natural modes of visual behavior. The difference might be attributed to the richness of the video stimuli, which include dynamic events, spatial layouts, color contrasts, and social interactions. This natural visual combination of features has seldom been incorporated into the study of face patch responses. It is also possible that active elements of vision that accompany free viewing, including exploration and attention, may unmask the different contribution of neural subpopulations (*32*). Regardless, the pronounced mixed selectivity observed during video viewing bears some resemblance to that measured in other regions across the brain (*33, 34*). It also presents practical challenges for systems and cognitive neuroscience, which often makes the tacit assumption of functional segregation in the brain.

At a more mechanistic level, it is interesting to speculate that the contrast between conventional and naturalistic testing derives from the engagement of different synaptic subpopulations providing input to individual cortical neurons. For example, during brief image presentation, a given neuron's selectivity to faces might be conferred by the simultaneous activation of a locally shared set of inputs concerned with the analysis of facial structure. These inputs are likely concentrated within the face patches and serve as the basis for their functional definition. However, under more naturalistic conditions, the same neuron's activity may be dominated by other, long-range connections with a sparser pattern of input among face patch neurons (see ref. (*35*) for similar ideas in different context), as well as the effects of neuromodulation during active behaviors (*36*).

Finally, combining natural conditions with novel readouts pushes researchers to explore new conceptual spaces for studying brain function. In departing from the usual practice of linking neural responses to specific visual features, less emphasis is placed on local representation and encoding and more on the physiological coordination of brain regions involved in a wide range of sensory and motor functions. The present findings underscore the value of intermodal mapping as a robust tool for characterizing neural activity during complex natural behavior, as well as the inherent value of combining controlled and naturalistic paradigms for the development of hypotheses and conceptual frameworks in systems neuroscience.

References and Notes

1. P. Grimaldi, K. S. Saleem, D. Tsao, Anatomical Connections of the Functionally Defined "Face Patches" in the Macaque Monkey. *Neuron* **90**, 1325–1342 (2016).
2. S. Moeller, W. A. Freiwald, D. Y. Tsao, Patches with links: a unified system for processing faces in the macaque temporal lobe. *Science* **320**, 1355–1359 (2008).
3. D. Y. Tsao, W. A. Freiwald, R. B. Tootell, M. S. Livingstone, A cortical region consisting entirely of face-selective cells. *Science* **311**, 670–674 (2006).
4. D. Y. Tsao, W. A. Freiwald, T. A. Knutsen, J. B. Mandeville, R. B. Tootell, Faces and objects in macaque cerebral cortex. *Nat Neurosci* **6**, 989–995 (2003).
5. N. Kanwisher, J. McDermott, M. M. Chun, The fusiform face area: a module in human extrastriate cortex specialized for face perception. *J Neurosci* **17**, 4302–4311 (1997).
6. C. C. Hung *et al.*, Functional mapping of face-selective regions in the extrastriate visual cortex of the marmoset. *J Neurosci* **35**, 1160–1172 (2015).
7. K. S. Weiner, K. Grill-Spector, The evolution of face processing networks. *Trends Cogn Sci* **19**, 240–241 (2015).
8. N. Kanwisher, G. Yovel, The fusiform face area: a cortical region specialized for the perception of faces. *Philos Trans R Soc Lond B Biol Sci* **361**, 2109–2128 (2006).
9. D. Y. Tsao, S. Moeller, W. A. Freiwald, Comparing face patch systems in macaques and humans. *Proc Natl Acad Sci U S A* **105**, 19514–19519 (2008).
10. W. A. Freiwald, D. Y. Tsao, Functional compartmentalization and viewpoint generalization within the macaque face-processing system. *Science* **330**, 845–851 (2010).
11. C. Fisher, Winrich A. Freiwald, Contrasting Specializations for Facial Motion within the Macaque Face-Processing System. *Current Biology* **25**, 261–266 (2015).
12. J. Taubert *et al.*, Parallel Processing of Facial Expression and Head Orientation in the Macaque Brain. *J Neurosci* **40**, 8119–8131 (2020).
13. J. K. Hesse, D. Y. Tsao, The macaque face patch system: a turtle's underbelly for the brain. *Nat Rev Neurosci* **21**, 695–716 (2020).
14. W. A. Freiwald, The neural mechanisms of face processing: cells, areas, networks, and models. *Curr Opin Neurobiol* **60**, 184–191 (2020).
15. D. Pitcher, L. G. Ungerleider, Evidence for a Third Visual Pathway Specialized for Social Perception. *Trends Cogn Sci* **25**, 100–110 (2021).
16. D. B. McMahon, B. E. Russ, H. D. Elnaiem, A. I. Kurnikova, D. A. Leopold, Single-unit activity during natural vision: diversity, consistency, and spatial sensitivity among AF face patch neurons. *J Neurosci* **35**, 5537–5548 (2015).
17. B. E. Russ, D. A. Leopold, Functional MRI mapping of dynamic visual features during natural viewing in the macaque. *Neuroimage* **109**, 84–94 (2015).
18. U. Hasson, Y. Nir, I. Levy, G. Fuhrmann, R. Malach, Intersubject synchronization of cortical activity during natural vision. *Science* **303**, 1634–1640 (2004).
19. D. Mantini *et al.*, Interspecies activity correlations reveal functional correspondence between monkey and human brain areas. *Nat Methods* **9**, 277–282 (2012).
20. A. G. Huth *et al.*, Decoding the Semantic Content of Natural Movies from Human Brain Activity. *Frontiers in Systems Neuroscience* **10**, (2016).
21. D. A. Leopold, J. F. Mitchell, W. A. Freiwald, in *Evolution of Nervous Systems (Second Edition),* J. H. Kaas, Ed. (Academic Press, Oxford, 2017), pp. 203–235.
22. D. A. Leopold, S. H. Park, Studying the visual brain in its natural rhythm. *Neuroimage* **216**, 116790 (2020).

23. I. V. Bondar, D. A. Leopold, B. J. Richmond, J. D. Victor, N. K. Logothetis, Long-term stability of visual pattern selective responses of monkey temporal lobe neurons. *PLoS One* **4**, e8222 (2009).
24. S. H. Park *et al.*, Functional Subpopulations of Neurons in a Macaque Face Patch Revealed by Single-Unit fMRI Mapping. *Neuron* **95**, 971–981 e975 (2017).
25. N. K. Logothetis *et al.*, Hippocampal-cortical interaction during periods of subcortical silence. *Nature* **491**, 547–553 (2012).
26. D. Barson *et al.*, Simultaneous mesoscopic and two-photon imaging of neuronal activity in cortical circuits. *Nat Methods* **17**, 107–113 (2020).
27. M. L. Scholvinck, A. Maier, F. Q. Ye, J. H. Duyn, D. A. Leopold, Neural basis of global resting-state fMRI activity. *Proc Natl Acad Sci U S A* **107**, 10238–10243 (2010).
28. A. Mitra, A. Z. Snyder, T. Blazey, M. E. Raichle, Lag threads organize the brain's intrinsic activity. *Proceedings of the National Academy of Sciences* **112**, E2235–2244 (2015).
29. J. L. Vincent *et al.*, Intrinsic functional architecture in the anaesthetized monkey brain. *Nature* **447**, 83–86 (2007).
30. N. Caspari, T. Janssens, D. Mantini, R. Vandenberghe, W. Vanduffel, Covert shifts of spatial attention in the macaque monkey. *J Neurosci* **35**, 7695–7714 (2015).
31. I. Sani, B. C. McPherson, H. Stemmann, F. Pestilli, W. A. Freiwald, Functionally defined white matter of the macaque monkey brain reveals a dorso-ventral attention network. *Elife* **8**, (2019).
32. C. E. Schroeder, D. A. Wilson, T. Radman, H. Scharfman, P. Lakatos, Dynamics of Active Sensing and perceptual selection. *Current Opinion in Neurobiology* **20**, 172–176 (2010).
33. S. Fusi, E. K. Miller, M. Rigotti, Why neurons mix: high dimensionality for higher cognition. *Curr Opin Neurobiol* **37**, 66–74 (2016).
34. A. C. Huk, L. N. Katz, J. L. Yates, The Role of the Lateral Intraparietal Area in (the Study of) Decision Making. *Annual Review of Neuroscience* **40**, 349–372 (2017).
35. T. Sato *et al.*, Object representation in inferior temporal cortex is organized hierarchically in a mosaic-like structure. *J Neurosci* **33**, 16642–16656 (2013).
36. C. J. Peck, C. D. Salzman, The amygdala and basal forebrain as a pathway for motivationally guided attention. *Journal of Neuroscience* **34**, 13757–13767 (2014).
37. D. B. T. McMahon, I. V. Bondar, O. A. T. Afuwape, D. C. Ide, D. A. Leopold, One month in the life of a neuron: longitudinal single-unit electrophysiology in the monkey visual system. *Journal of Neurophysiology* **112**, 1748–1762 (2014).
38. K. W. Koyano *et al.*, Dynamic Suppression of Average Facial Structure Shapes Neural Tuning in Three Macaque Face Patches. *Curr Biol* **31**, 1–12.e15 (2021).
39. A. P. Khandhadia, A. P. Murphy, L. M. Romanski, J. K. Bizley, D. A. Leopold, Audiovisual integration in macaque face patch neurons. *Current Biology*, (2021).
40. J. Hwang, A. R. Mitz, E. A. Murray, NIMH MonkeyLogic: Behavioral control and data acquisition in MATLAB. *J Neurosci Methods* **323**, 13–21 (2019).
41. R. W. Cox, AFNI: software for analysis and visualization of functional magnetic resonance neuroimages. *Comput Biomed Res* **29**, 162–173 (1996).
42. Q.-S. Xiang, F. Q. Ye, Correction for geometric distortion and N/2 ghosting in EPI by phase labeling for additional coordinate encoding (PLACE). *Magnetic Resonance in Medicine* **57**, 731–741 (2007).
43. D. C. Van Essen *et al.*, An integrated software suite for surface-based analyses of cerebral cortex. *J Am Med Inform Assoc* **8**, 443–459 (2001).
44. R. Q. Quiroga, Z. Nadasdy, Y. Ben-Shaul, Unsupervised spike detection and sorting with wavelets and superparamagnetic clustering. *Neural Comput* **16**, 1661–1687 (2004).

45. A. H. Bell *et al.*, Relationship between Functional Magnetic Resonance Imaging-Identified Regions and Neuronal Category Selectivity. *The Journal of Neuroscience* **31**, 12229 (2011).
46. P. L. Aparicio, E. B. Issa, J. J. DiCarlo, Neurophysiological Organization of the Middle Face Patch in Macaque Inferior Temporal Cortex. *The Journal of Neuroscience* **36**, 12729 (2016).
47. E. B. Issa, J. J. DiCarlo, Precedence of the eye region in neural processing of faces. *J Neurosci* **32**, 16666–16682 (2012).

Acknowledgments: We thank Katy Smith and Julie Hong for assistance with data collection and members in the Leopold lab for helpful comments. Functional and anatomical MRI scanning was carried out in the Neurophysiology Imaging Facility Core (NIMH, NINDS, NEI). This work utilized the computational resources of the NIH High Performance Computing Core (https://hpc.nih.gov/).

Funding:

Intramural Research Program of the National Institute of Mental Health ZIAMH002838 and ZIAMH002898

Korea Health Technology R&D Project through the Korea Health Industry Development Institute (KHIDI) funded by the Ministry of Health & Welfare grant HI14C1220 (SHP)

Author contributions:

Conceptualization: SHP, DAL

Data curation: SHP

Formal Analysis: SHP, KWK, BER, ENW, DBTM

Funding acquisition: DAL

Investigation: KWK, BER, ENW, DBTM

Methodology: SHP, KWK, BER, DBTM

Supervision: DAL

Visualization: SHP

Writing – original draft: SHP, DAL

Writing – review & editing: SHP, KWK, BER, ENW, DBTM, DAL

Competing interests: Authors declare that they have no competing interests.

Data and materials availability: The datasets generated and/or analyzed during the current study are available from the corresponding author on reasonable request.

Supplementary Materials

Materials and Methods

Figs. S1 to S5

References (*37–47*)

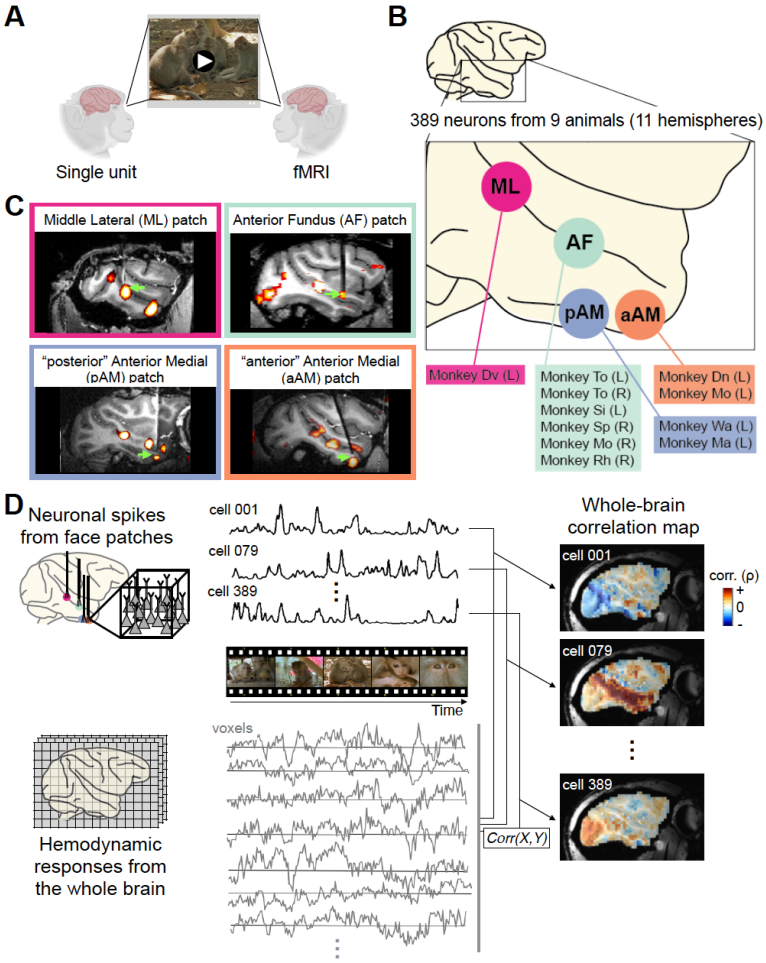

Fig. 1. Computing whole-brain correlation maps for individual neurons from four face patches. (**A**) Schematic diagram of experimental paradigm. Two cohorts of animals freely and repeatedly viewed the same set of naturalistic videos, during single unit recording and fMRI acquisition, respectively. The two measures of neural activity could be directly correlated, as the responses of both were synchronized to the same video content. (**B**) Schematic diagram of microwire bundle recording locations in this study, in all cases introduced into fMRI-identified of face patches. Animal identifications for each face patch recording are listed with hemispheric information in parenthesis. Abbreviation for face patches: ML, middle lateral; AF, anterior fundus; pAM, posterior part of anterior medial; aAM, anterior part of anterior medial. (**C**) Representative MR images showing recording electrode in each face patch. **(D)** Basic multimodal analyses underlying single-unit fMRI mapping. The time series corresponding to each neuron's spiking fluctuations was correlated with that of fMRI voxels throughout the brain, after adjusting for the hemodynamic response profile (see **Materials and Methods**). Representative examples of single-unit correlation maps from three different neurons are shown on a sagittal section on the right. Panel (A) is created with BioRender.com.

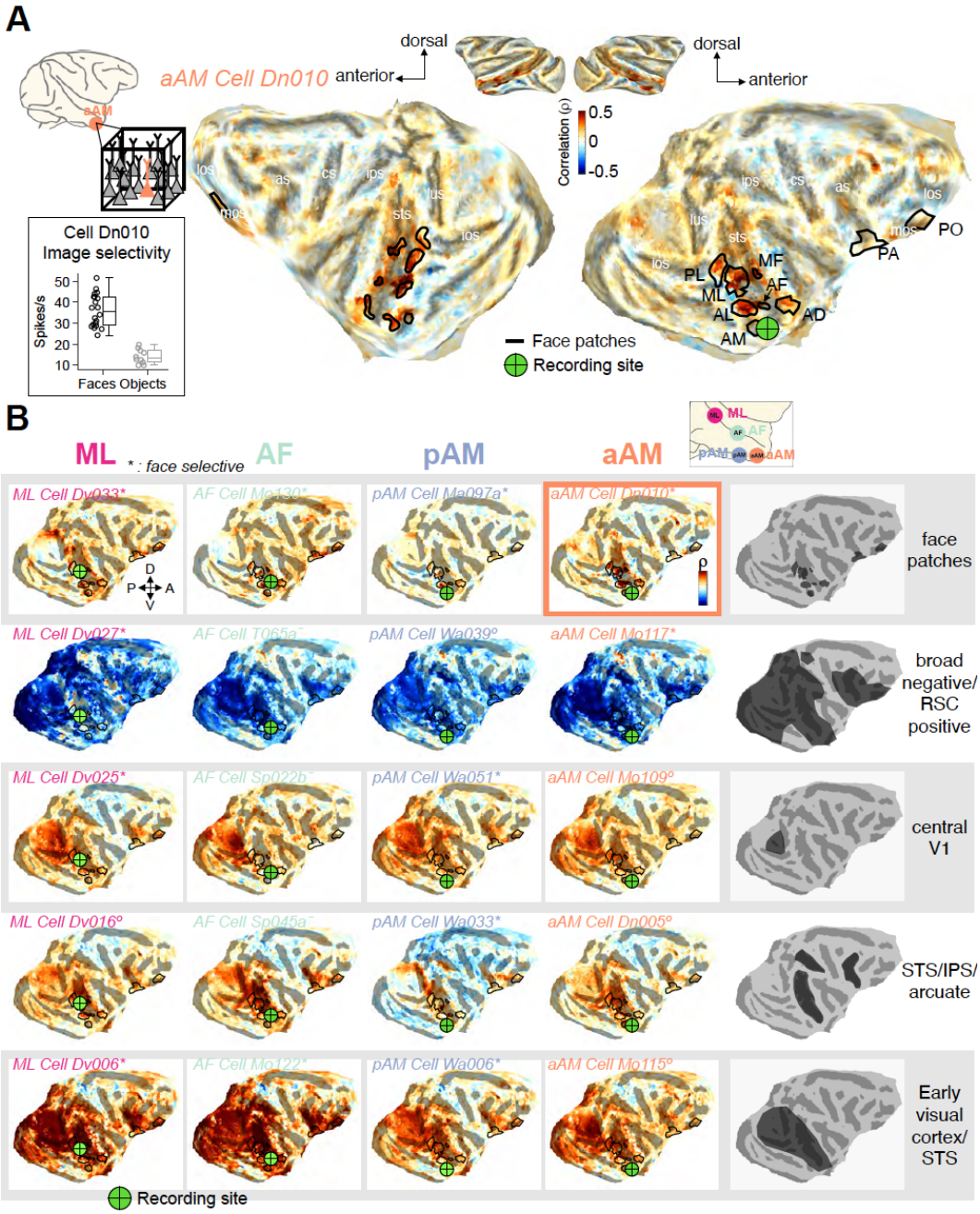

Fig. 2. Examples of single-unit fMRI maps from neurons in four face patches. Cortical fMRI correlation pattern of example neurons recorded from four face patches projected onto the flattened cortical surface of one animal's brain. Small green cross on each map indicates the location of recording site of the featured neuron. Location of face patches (black lines) are based on separate fMRI block design experiments. Abbreviation for face patches: PL, posterior lateral; ML, middle lateral; MF, middle fundus; AL, anterior lateral; AF, anterior fundus; AM, anterior medial; AD, anterior dorsal; PA, prefrontal arcuate; PO, prefrontal orbital face patch. (**A**) Correlation map of an example neuron from face patch aAM. Inset, spiking responses to brief presentations of faces (n = 20) and nonface objects (n = 10) demonstrate that this neuron is face selective. Center line, median; box limits, upper and lower quartiles; whiskers, range. lus, lunate sulcus; ios, inferior occipital sulcus; sts, superior temporal sulcus; ips, intraparietal sulcus; cs,

central sulcus; as, arcuate sulcus; los, lateral orbital sulcus; mos, medial orbital sulcus. (**B**) Maps of 20 example neurons (cell identity is written in italics) from four face patch recording sites, presented in a matrix format. Each column of the matrix contains five neurons from each local recording site, face patches ML, AF, pAM, and aAM (from left to right), whose fMRI maps differ substantially. Each row shows fMRI maps with similar features that were common to neurons across all four recording sites, with the specific features summarized on the right. Based on separate testing, asterisks indicate neurons that were face selective, circles those that were not face selective, and dashes those that were not tested (see **Materials and Methods**). Map of the example neuron in (A) is marked with an outline. RSC, retrosplenial cortex.

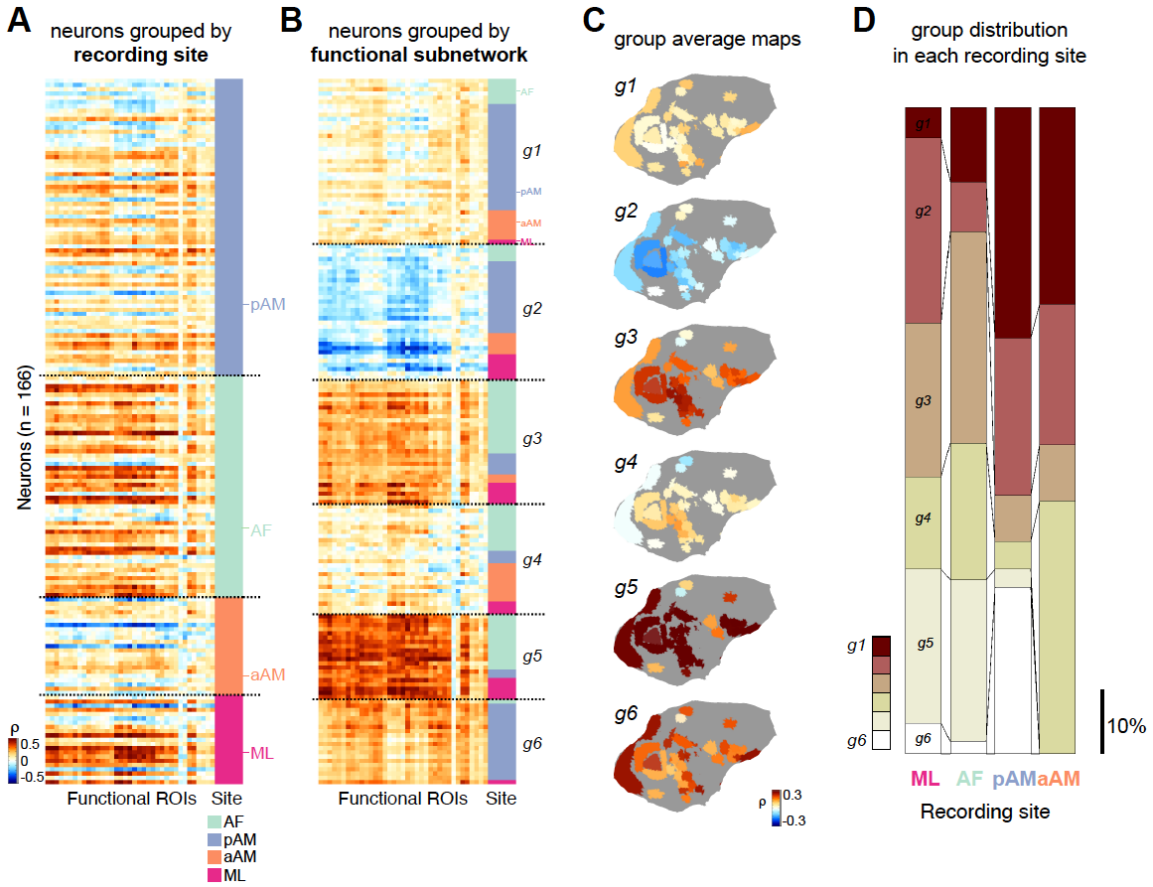

Fig. 3. Distinct cortical correlation patterns distributed across spatially remote face patches. (**A**) fMRI correlation profiles of spiking activity from verified face-selective neurons (row; n = 166) across 37 functional regions of interest in the cerebral cortex (fROIs; see **Materials and Methods** and **Fig. S3**) (column; n = 37 from fROI 1 to fROI 37, from left to right). Each row is a 37-element vector of fROI correlation coefficients stemming from one neuron. Neurons are grouped by face patch recording location, indicated on the right in different colors. (**B**) Same format as (A), but with neurons sorted into groups *g1* – *g6* according to their functional clustering (see **Materials and Methods**). (**C**) Neural fMRI correlation profiles from (B) averaged across neurons in each group and mapped spatially onto the original fROIs on the cortical surface. (**D**) Proportion of neurons belonging to each cell group found at each of the recorded face patches. Color indicates identity of cell groups from (B) and (C). Scale bar indicates 10% of proportion.

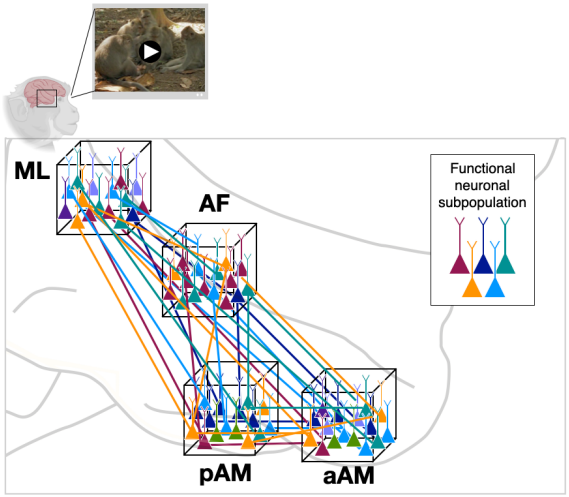

Fig. 4. Parallel functional subnetworks pervading the face patch system. Schematic diagram depicting functionally distinct subnetworks operating in parallel within the face processing network. Local cell populations are indicated by neurons within each of the cubes, corresponding to the four face patches recorded in the present study. Coloration indicates functionally distinct classes of neurons. The sharing of distinct functional operations across face patches, and the mixing of such signals locally, were central observations in the present study. The selective long-range connections among functionally similar classes of neurons (colored lines) are hypothesized.